Food Chemistry: X 20 (2023) 100966

Contents lists available at ScienceDirect

Food Chemistry: X

journal homepage: www.sciencedirect.com/journal/food-chemistry-x

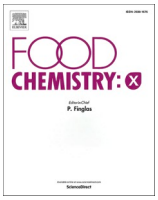

Identification of metabolite biomarkers in *Salmonella enteritidis*-contaminated chickens using UHPLC-QTRAP-MS-based targeted metabolomics

Lan Chen [a,c,e], Tao Zhang [b,c], Hao Ding [a,c], Xing Xie [d], Yali Zhu [b,c], Guojun Dai [b,c], Yushi Gao [a,d], Genxi Zhang [b,c,*], Kaizhou Xie [a,b,c,*]

[a] College of Veterinary Medicine, Yangzhou University, Yangzhou 225009, China
[b] College of Animal Science and Technology, Yangzhou University, Yangzhou 225009, China
[c] Joint International Research Laboratory of Agriculture & Agri-Product Safety of MOE, Yangzhou University, Yangzhou 225009, China
[d] Institute of Veterinary Medicine, Jiangsu Academy of Agricultural Sciences, Key Laboratory of Veterinary Biological Engineering and Technology, Ministry of Agriculture, Nanjing 210000 China
[e] Poultry Institute, Chinese Academy of Agricultural Sciences, Yangzhou 225009, China

ARTICLE INFO

Keywords:
S. enteritidis
Chicken
UHPLC-QTRAP-MS
Metabolite biomarkers

ABSTRACT

This study aimed to characterize the metabolic profile of *Salmonella enteritidis* (*S. enteritidis*) in chicken matrix and to identify metabolic biomarkers of *S. enteritidis* in chicken. The UHPLC-QTRAP-MS high-throughput targeted metabolomics approach was employed to analyze the metabolic profiles of contaminated and control group chickens. A total of 348 metabolites were quantified, and the application of deep learning least absolute shrinkage and selection operator (LASSO) modelling analysis obtained eight potential metabolite biomarkers for *S. enteritidis*. Metabolic abundance change analysis revealed significantly enriched abundances of anthranilic acid, l-pyroglutamic acid, 5-hydroxylysine, n,*n*-dimethylarginine, 4-hydroxybenzoic acid, and menatetrenone in contaminated chicken samples. The receiver operating characteristic (ROC) curve analysis demonstrated the strong ability of these six metabolites as biomarkers to distinguish *S. enteritidis* contaminated and fresh chicken samples. The findings presented in this study offer a theoretical foundation for developing an innovative approach to identify and detect foodborne contamination caused by *S. enteritidis*.

1. Introduction

S. enteritidis is an important zoonotic pathogen that seriously threatens animal husbandry and human health (Regalado-Pineda, Rodarte-Medina, Resendiz-Nava, Saenz-Garcia, Castaeda-Serrano, & Nava, 2020). The contamination caused by *S. enteritidis* has become the main cause of bacterial food poisoning in China and even in the world (Castro-Vargas, Herrera-Sánchez, Rodríguez-Hernández, & Rondón-Barragán, 2020). According to the Global Burden of Disease, Injury and Risk Factor Study (GBD), *S. enteritidis* caused 95.1 million cases of illness, 3.1 million labour force losses, and 50,771 deaths in 2017 (Parisi, Stanaway, Sarkar, & Crump, 2020). The European Union estimates annual losses from *Salmonella* at more than three billion euros.

Chicken, characterized by high protein, low fat, low cholesterol, and low calories, has developed into the world's largest meat consumer product (Chen et al., 2023). Due to the impact of H7N9 influenza on poultry, live poultry trading has been restricted or banned in Asian countries in recent years (Zhang et al., 2021). Policies such as targeted slaughtering, cold-chain transport and the marketing of fresh chilling have been implemented (Wang et al., 2022). Importantly, fresh chicken is considered to be one of the major exposures of humans to *S. enteritidis* (Antunes, Mourão, Campos, & Peixe, 2016), and approximately 30 % of foodborne *salmonellosis* may be related to poultry meat (Sandra et al., 2017). To protect national safety, it is necessary to prevent *S. enteritidis* contamination of fresh chicken and meat products in the food chain to limit human transmission while extending the shelf life and reducing economic losses. Therefore, monitoring and conducting premarket detection for *S. enteritidis* contamination during chicken production is

* Corresponding authors at: College of Animal Science and Technology, Yangzhou University, 48 East Wenhui Road, Yangzhou 225009, Jiangsu, China.
E-mail addresses: zhangt@yzu.edu.cn (T. Zhang), gjdai@yzu.edu.cn (G. Dai), gaoys100@sina.com (Y. Gao), gxzhang@yzu.edu.cn (G. Zhang), yzxkz168@163.com (K. Xie).

https://doi.org/10.1016/j.fochx.2023.100966
Received 29 April 2023; Received in revised form 21 October 2023; Accepted 24 October 2023
Available online 27 October 2023

essential. Currently, the detection methods of *S. enteritidis* mainly include the traditional conventional culture method, immunology, biosensors, molecular biology technology, and other rapid detection methods. However, although the traditional culture method is the gold standard, it has high accuracy and strong selectivity, the inspection cycle is relatively long, and the operation is cumbersome, resulting in limited optimal detection time. Nonspecific adsorption of biosensors will affect the accuracy of detection results, immunoassays require specific antibodies, and PCRs are always restricted by power, cost, space and other factors (Kamarudin, Cox, & Kolamunnage-Dona, 2017; Song, Li, Duan, Li, & Deng, 2014; Wu et al., 2014). Therefore, it is not easy to achieve rapid field detection of pathogens, which cannot meet the requirements of modern foodborne pathogen detection.

Metabolomics is the study of all low-molecular-weight (<1500 Da) metabolites of tissues or cells in a certain physiological period (Bover-Cid, Izquierdo-Pulido, & Vidal-Carou, 2000). This technique has been widely used in clinical diagnosis, medicine, microbial metabolism, food science, animal husbandry, and other fields (Johnson, Ivanisevic, & Siuzdak, 2016; Lechtenfeld, Hertkorn, Shen, Witt, & Benner, 2015; Pinu et al., 2019; Slowinska, Sallem, Clench, & Ciereszko, 2018; Wen, Liu, & Yu, 2020). With the development of the economy and the continuous improvement of food quality standards, metabolomics has been developed to comprehensively evaluate the quality and safety of food and provide valuable information for the quality and authenticity of food (Jadhav et al., 2019). *S. enteritidis* can produce many low-molecular-weight metabolites after contaminating chickens. Hence, metabolomic assays can be used to analyse the metabolic profile of *S. enteritidis* and excavate biomarkers, laying the foundation for developing new detection methods (Cevallos-Cevallos, Reyes-De-Corcuera, Etxeberria, Danyluk, & Rodrick, 2009). For example, Xu et al. identified 17 metabolic markers using metabonomics and bioinformatics analysis to distinguish *Salmonella* typhimurium-contaminated pork from naturally deteriorated pork (Yun, Cheung, Winder, Dunn, & Goodacre, 2011). Based on metabonomics technology, Manuel et al. established a rapid detection method for *Escherichia coli* O157:H7 and *Salmonella* in beef and chicken (Manuel & Danyluk, 2011).

High-throughput targeted metabolomics is a new metabolome detection technology that integrates the "universality" of nontargeted metabolomics and the "accuracy" of targeted metabolomics, featuring advantages of high throughput, high sensitivity, comprehensive coverage, absolute qualitative and quantitative. More abundant, precise, and effective metabolites can be mined using targeted metabolomics (Schrimpe-Rutledge, Codreanu, Sherrod, & Mclean, 2016). This study used the targeted metabolomics technique of UHPLC-QTRAP-MS to characterize the metabolic profile of *S. enteritidis* in the chicken matrix. Then, the orthogonal partial least squares discriminant analysis (OPLS-DA) model and LASSO were employed to examine the differences in metabolites between fresh chicken and *S. enteritidis*-contaminated chicken samples, thereby identifying potential metabolite biomarkers of *S. enteritidis* in chicken. The ROC analysis was used to identify and evaluate the reliability of potential metabolite biomarkers. This result provides a theoretical basis for developing new methods for rapidly and accurately detecting *S. enteritidis*-contaminated chicken.

2. Materials and methods

2.1. Materials and reagents

Acetonitrile (CAS: 75–05-8), methanol (CAS: 67–56-1) and aqueous ammonia (CAS: 631–61-8) were all of chromatographic purity grade and were provided by CNW Technologies Co., Germany. Ammonium acetate (CAS: 631–61-8) was analytically pure and was purchased from Sigma-Aldrich in the USA.; LB broth medium and xylose lysine desoxycholate agar were obtained from Hopebio Corp. (China); a high-speed refrigerated centrifuge (Thermo Fisher Corp., USA), an ACQUITY UPLC H-Class instrument (Waters Corp., USA), and a 6500 plus QTRAP triple quadrupole mass spectrometer (AB Sciex, USA) were used in this study; an Atlantis Premier BEH Z-HILIC column (1.7 μm, 2.1 mm *150 mm, Waters Corp., USA) was also used. The deionized water used in the test was all prepared by Milli-Q system (Millipore, USA).

2.2. Sample preparation

Chilled chicken breast tissue was purchased from Jiangsu Sushi Meat Co., Ltd. and was refrigerated and transported to an ultraclean workbench in the laboratory in half an hour. In a sterile environment, the sample was immediately divided into an experimental and control group, each weighing 25 ± 0.2 g. Background bacteria in the chicken samples were removed using PBS cleaning + UV lamp irradiation, and each sample was then packed into sterile plastic bags. The experimental group samples were inoculated with 1 mL (2–3 log CFU/mL) of *S. enteritidis* suspension (General Microbiological Culture Collection Center, China), mixed well and sealed. Fresh chicken samples without inoculated liquid were used as the blank control group (BG). All samples were cultured in constant-temperature incubators (n = 10) immediately after sampling and numbering, quenched in liquid nitrogen for 10 min and stored at −80 °C.

2.3. Metabolite extraction

Approximately 50 ± 0.2 mg of each chicken sample was weighed, and 1000 μL of acetonitrile/methanol/H2O (4:4:1, including internal isotope standard) extract solution was added and mixed with two magnetic beads. Samples were homogenized at 35 Hz for 4 min, sonicated in an ice-water bath for 5 min, repeatedly homogenized and sonicated 3 times, and incubated at −40 °C for 2 h. Then, the samples were centrifuged at 12000 rpm and 4 °C for 15 min. A total of 800 μL supernatant of each sample was transferred to a new Eppendorf tube and dried with a centrifugal concentrator. Then, 160 μL of 60 % acetonitrile was added to the Eppendorf tube to reconstitute the dried samples. The Eppendorf tube was vortexed until the powder was dissolved, followed by centrifugation at 12000 rpm and 4 °C for 15 min. Finally, 100 μL supernatant of each sample was transferred to a glass vial for LC-MS/MS analysis.

2.4. UHPLC-QTRAP-MS analysis

LC separation was carried out using a UPLC System (H-Class, Waters) equipped with a Waters Atlantis Premier BEH Z-HILIC Column (1.7 μm, 2.1 mm *150 mm). Mobile phase A was mixed with H_2O and acetonitrile (8:2) containing 10 mmol/L ammonium acetate, and mobile phase B was composed of H_2O and acetonitrile (1:9) containing 10 mmol/L ammonium acetate. Mobile phases A and B were adjusted to pH 9 with aqueous ammonia. The column temperature was set at 40 °C. The autosampler temperature was 8 °C, and the injection volume was 1 μL. The complete analysis contained 348 metabolites, mainly including 13 classifications. The quantification of metabolites was carried out by the standard external method and corrected with the internal standard of the isotope. The stability and functionality of the system are quality controlled by instrument analysis (He et al., 2022).

An AB Sciex QTRAP 6500 + mass spectrometer was applied for all multiple-reaction monitoring experiments for assay development. Typical ion source parameters were as follows: ionspray voltage, +5000 V/-4500 V; curtain gas, 35 psi; temperature, 400 °C; ion source gas 1, 50 psi; and ion source gas 2, 50 psi (Zhang, Mu, Shi, & Zheng, 2022).

2.5. Quality control (QC)

The testing process uses the solution of all samples mixed in equal amounts as the QC sample. One QC sample was inserted every ten samples to ensure the stability and repeatability of the testing and analysis process. When an internal isotope standard with the same

concentration is introduced into QC samples, the response difference should be less than 15 % (Sangster, Major, Plumb, Wilson, & Wilson, 2006).

2.6. Linearity and range

Linearity is usually expressed using a linear regression equation to obtain a correlation between analyte concentrations and test response values. In this experiment, the linear relationship between the eight concentration levels of the polar metabolites and the peak area was determined, and the linear regression of the concentrations was performed using the least squares method with the mean peak area to obtain the linear regression equation and calculate the linear relationship (R^2). The standard curves for the metabolites were plotted according to the linear regression equation, with the high and low concentration ranges being linear.

2.7. Quantification of metabolites

UHPLC-QTRAP-MS collected the original data and annotated all peaks to obtain qualitative and quantitative information. The standard curve method was used to calculate the abundance of each metabolite. All data were merged using an internal macro program in Microsoft Excel 2016 (Microsoft Corp, Redmond, WA, USA)(Leng et al., 2022).

2.8. Data processing and multivariate data analysis

First, ProteoWizard was used to convert the original data into mzXML format. XCMS software (version 1.0) was used for processing, including baseline correction, denoising, deconvolution, and peak alignment. Individual metabolites were filtered. Only metabolite data were retained with no more than 50 % empty values in one group or no more than 50 % empty values in all groups, and missing values were recorded in the original data (the numerical simulation method was filled with half of the minimum value). The preprocessing results generate a data matrix of retention time, mass-to-charge ratio (m/z) and peak intensity. The fold change (FC) for each metabolite between the groups of *S. enteritidis*-contaminated chicken and fresh chicken samples was calculated. The data matrix was imported into SIMCA software (V16.0.2, Sartorius Stedim Data Analytics AB, Umea, Sweden), and LOG conversion or par formatting was performed. After these transformations, principal component analysis (PCA) was carried out to visualize the distribution. The grouping of the samples, OPLS-DA automatic modelling analysis and Student's t test were conducted to obtain variable importance in the projection (VIP) value and p value (Lindon, Holmes, & Nicholson, 2006; Trygg & Wold, 2002; Wiklund et al., 2008). To identify statistically significant metabolites, volcano plots were displayed for differentially abundant metabolites using univariate statistical methods (Xia & Wishart, 2016).

A self-built R package (Version 3.6.3) was used to visualize metabolites. MetaboAnalyst 5.0, based on the Kyoto Encyclopedia of Genes and Genomes (KEGG) metabolic pathway library, was used for pathway analysis of all statistically significant metabolites. As a machine learning method, the LASSO analysis refines the variable selection and regularization from a large number of potential multicollinearity variables (Algamal & Lee, 2015; Dyar et al., 2012; Mceligot, Poynor, Sharma, & Panangadan, 2020; Soh & Zhu, 2022). Furthermore, a more relevant and interpretable LASSO model was generated using the LASSO algorithm to mine metabolite biomarkers (Chen, Feng, Dai, Xudong, Zhou, Chang Chun, Li, Ke Xin, Zhang, Yu Juan, Lou, Xiao Ying, Cui, Wei %J Gut: Journal of the British Society of Gastroenterology. (2022), 2022). he t test was used to assess the difference in the abundance of metabolite biomarkers between the two groups, with $P < 0.05$ as the significance criterion. ROC curve analysis was used to evaluate the sensitivity and specificity of metabolite biomarkers discriminant ability.

3. Results and discussion

3.1. Linearity and range

The mixed standard solutions were diluted step by step. The peak areas of the target metabolites in the samples were detected and regressed against the injection volume using the peak areas. The results are presented in Table S1, showing the lower limit of quantification (LLOQ), the upper limit of quantification (ULOQ), the linear regression equation, and the R^2 for the 348 metabolites. The R^2 values of the standard metabolite curve were all greater than 0.99, indicating an excellent linear relationship (Schmidt et al., 2016).

3.2. Metabolic profile and data analysis

Based on the UHPLC-QTRAP-MS targeted metabolomics, the metabolites of chicken samples from *S. enteritidis*-contaminated and blank control groups were studied. We compared the total ion flow diagrams of QC samples by overlapping the spectra. As shown in Fig. 1A, the baseline of the QC samples was stable. Each chromatogram peak's corresponding intensities and retention times were the same, indicating that the variation caused by instrument error was small in the test process and that the data quality was stable and reliable. As shown in Fig. 1B, the total ion flow diagrams of samples from the *S. enteritidis*-contaminated group and the fresh control group are different, indicating differences in the composition of metabolites between the two groups (Zhang, Yang, Huang, & Gao, 2019). The quality control results are shown in Fig. 1C-D. The standard deviation of the samples was within ± 2 STD, and the correlations between QC samples were greater than 0.9. Moreover, the RSD value of the standard internal response in QC samples was less than 15 % (Table S2). The above results indicated that the instrument system is stable and that the obtained experimental data are reliable. SIMCA software was used to reduce the dimension of the original complex data, and the feature that contributes most to the difference in the dataset was maintained for PCA automatic modelling analysis (A. E. Johnson, Sidwick, Pirgozliev, Edge, & Thompson, 2018). The PCA results of the *S. enteritidis*-contaminated group and the control group are shown in Fig. 1E. All samples were within a 95 % confidence interval, with the contribution rates of the first principal component (PC1) and the second principal component (PC2) being 67.9 % and 5.8 %, respectively. Clustering samples from the same group indicates good repeatability between samples, while the distance between samples from different groups is relatively long, indicating significant differences.

Qualitative and quantitative analyses were conducted on the metabolites of chicken samples from the *S. enteritidis* contamination group and the blank control group. Three hundred forty-eight metabolites were identified and divided into 14 categories: amino acids, polypeptides and analogues, nucleosides and nucleotides and analogues, carbohydrates and carbohydrate conjugates, organic acids and organic acids and derivatives, biogenic amine and benzene (Table S3).

Amino acids, polypeptides and analogues were the most abundant metabolites, with 101 observed, accounting for 29 % of all metabolites (Fig. 1F, Fig. 2A). The concentrations of l-pyroglutamic acid, 5-hydroxylysine and n,*n*-dimethylarginine were significantly higher in the *S. enteritidis*-contaminated group than in the blank control group. Nucleosides, nucleotides and analogues were the second most abundant metabolites, with 53 detected, accounting for 15 % of all metabolites (Fig. 1F, Fig. 2B). We found that metabolites associated with meat deterioration, such as inosine, inosine acid, and uridine, clearly clustered the samples into two groups. Carbohydrates and carbohydrate conjugates were the third most abundant metabolites, with 46 detected, accounting for 13 % of all metabolites (Fig. 1F, Fig. 2C). We found that metabolites such as D-glucose, gluconic acid and gluconolactone clustered the samples into two groups. Fig. 2 displays the abundance of the 348 metabolites belonging to 14 categories across 20 samples.

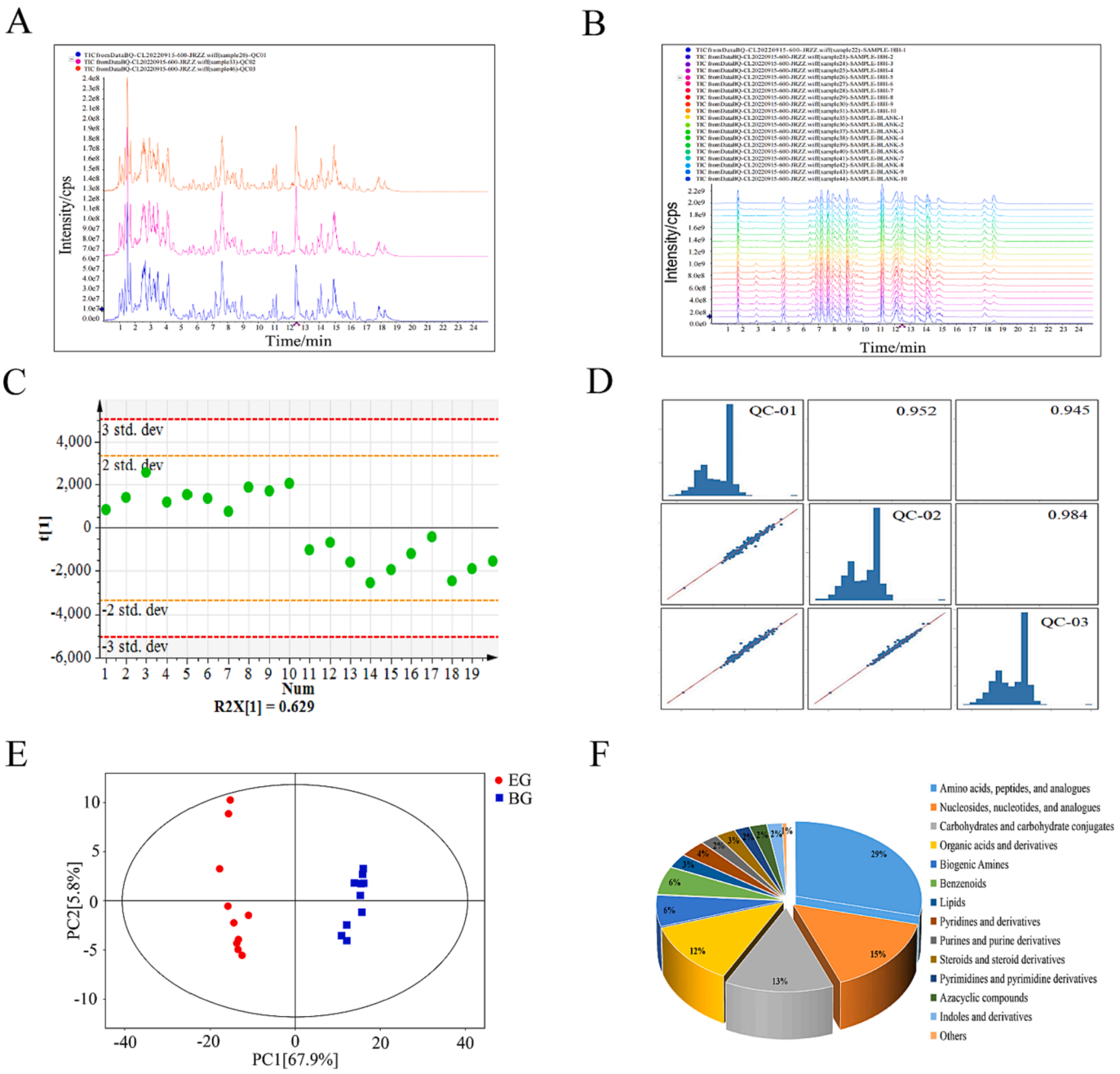

Fig. 1. Quality control of the experimental data, PCA of experimental samples and pie plot analysis of metabolite classification. (A) TIC plot of the QC sample, (B) TIC plot of the experimental samples, (C) Standard deviation of samples, (D) Correlation of QC sample, (E) PCA score plots, (F) Pie plots.

3.3. Identification of differentially abundant metabolites (DAMs)

DAMs were identified using fold change > 1 and *P* value < 0.05. The DAMs between the control and *S. enteritidis*-contaminated groups were visualized by a volcano plot (Fig. 3A). In total, 152 DAMs were identified by comparing *S. enteritidis*-contaminated samples vs. blank control samples, including 115 upregulated and 37 downregulated metabolites.

3.4. OPLS-DA

We constructed an OPLS-DA model to identify potential metabolite biomarkers for *S. enteritidis* contamination in chicken samples. OPLS-DA can remove irrelevant information after orthogonal signal correction, which is helpful for sample classification and irrelevant noise information in the dataset (Chang, Wu, Kan, Lin, & Liao, 2021). As shown in Fig. 3B, the OPLS-DA score plot separated the two groups of samples ($R^2X = 0.572$, $Q^2 = 0.983$), indicating that *Salmonella* contamination significantly altered the metabolic profile of the samples. A 200 permutation test was carried out to evaluate the validity of the OPLS-DA model (Zhou et al., 2022). The results show that, as shown in Fig. 3C-D, a high R^2Y of 0.998 and a Q^2 of 0.983 were achieved. The slope of the regression line is large, the intercept of the fitted curve of Q^2 on the Y-axis is less than 0, and R2Y is $P < 0.05$, indicating that the model is robust and has good stability and predictability. The results above indicated that the fitted OPLS-DA model has a goodness-of-fit and high prediction ability. According to the predicted VIP > 1, $P < 0.05$ and FC > 1, 152 DAMs were screened (Table 1).

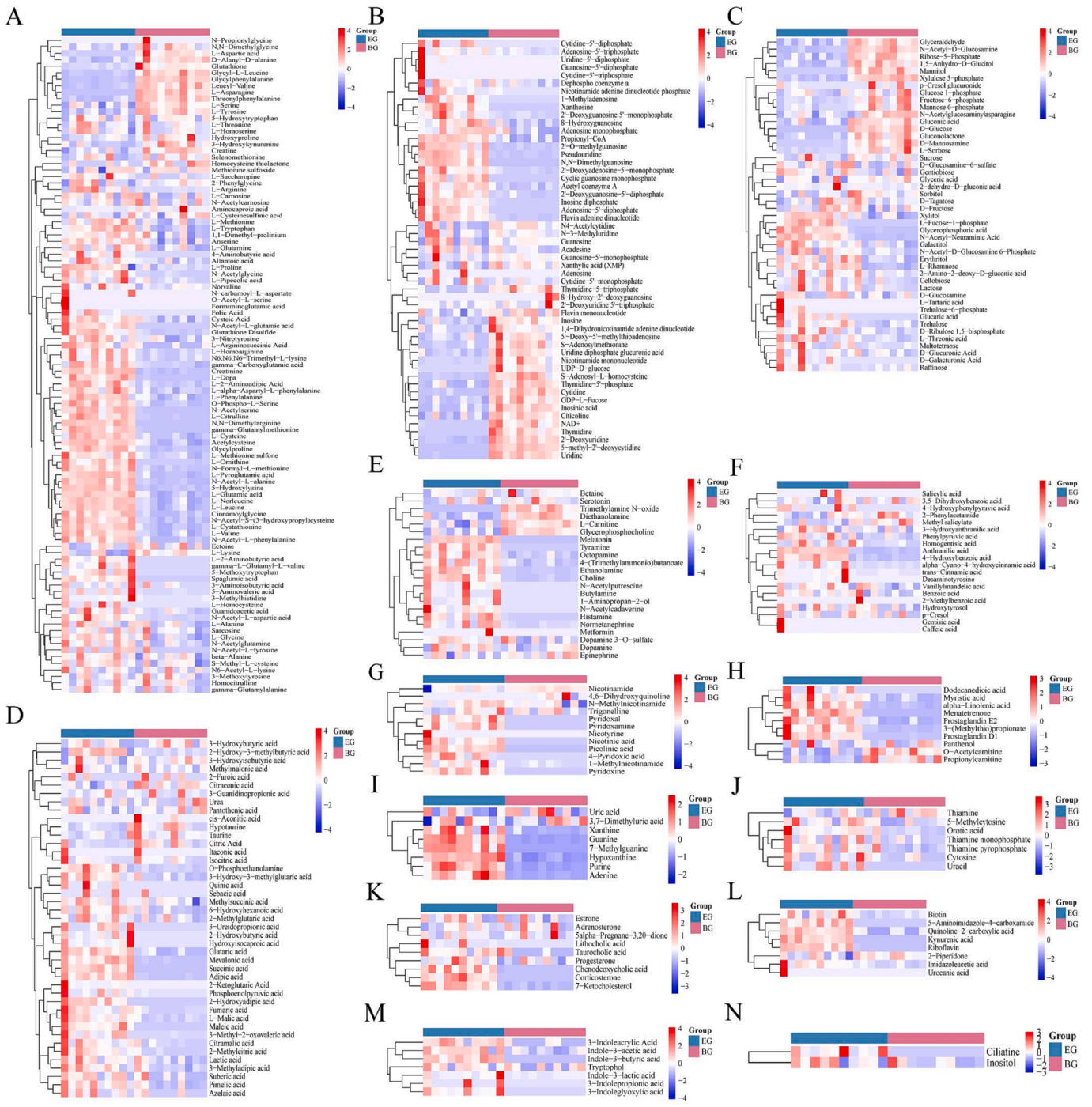

Fig. 2. Heatmap of the abundance of the 348 metabolites belonging to 14 categories across 20 samples.

3.5. Metabolic pathway enrichment analysis of DAMs

MetaboAnalyst 5.0 was used for pathway enrichment analysis. As shown in Fig. 3E, 152 DAMs were significantly enriched in eight metabolic pathways, including alanine, aspartate and glutamate metabolism, vitamin B6 metabolism, arginine and proline, purine metabolism, glutathione metabolism, ascorbate and aldarate metabolism, phenylalanine, tyrosine and tryptophan biosynthesis and aminoacyl-tRNA biosynthesis. Amino acid metabolism is reported to be involved in chicken spoilage, while purine metabolism plays an important role in the degradation of raw meat and meat (Dario, Gaston, Robledo, & Susana. , 2018; Jadhav et al., 2018). We can infer that these eight metabolic pathways are more closely related to *S. enteritidis*-contaminated chicken meat and that l-hydroxylysine, melatonin and anthranilate are enriched in the amino acid metabolic pathway and may be important metabolites in *S. enteritidis*-contaminated chickens.

3.6. LASSO analysis

To differentiate *S. enteritidis*-contaminated chicken samples from control chicken samples, the experiments were analysed with LASSO using the cv. glmnet function from the glmnet package (version 4.1.8) with a minimum error lambda value of 0.000605 and a 1-SE value of 0.001057, and after 200 iterations, eight independent effect metabolites were identified (Table S4). Fig. 3F-H shows that anthranilic acid, l-pyroglutamic acid, 5-hydroxylysine, n,*n*-dimethylarginine, 4-

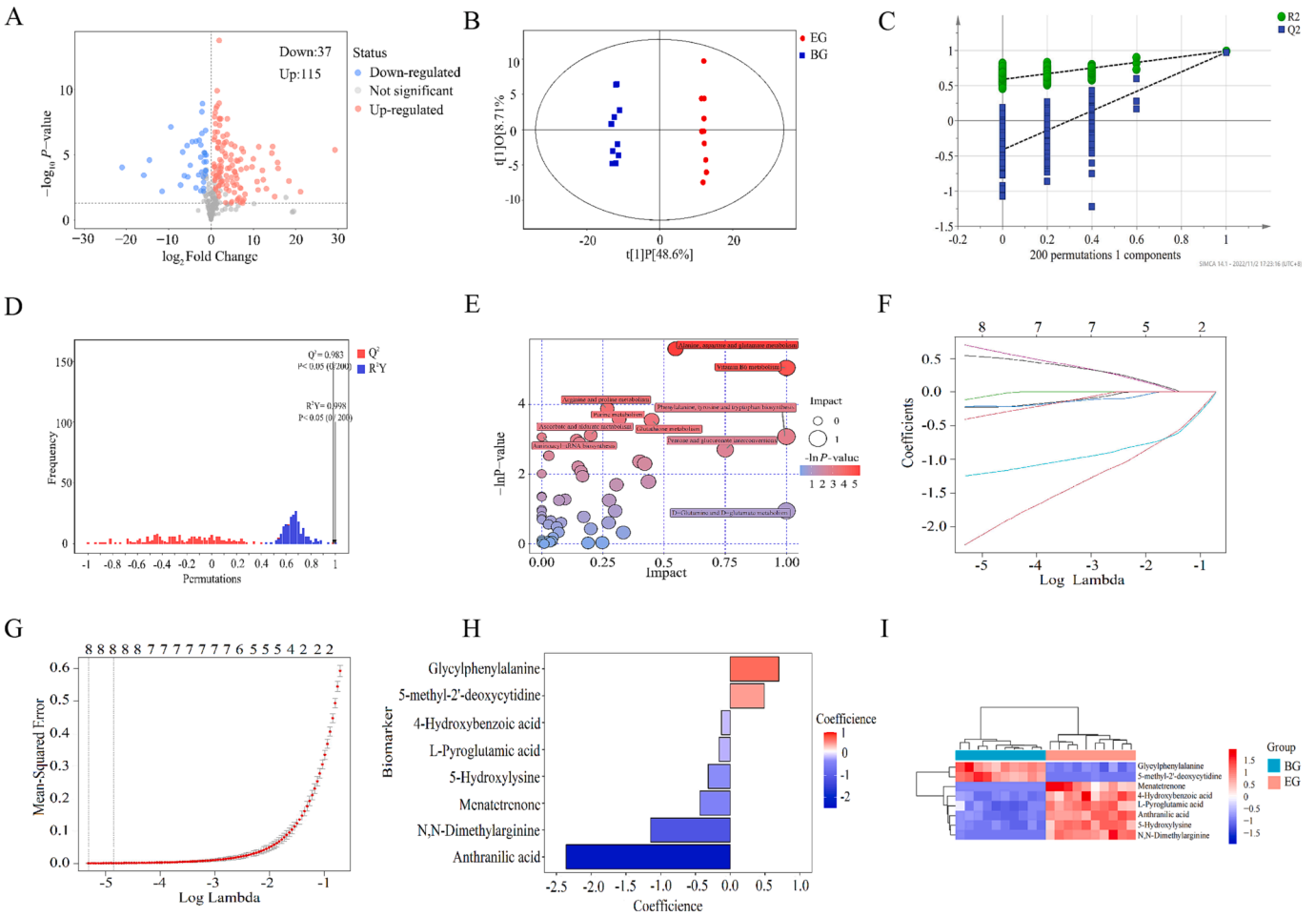

Fig. 3. Identification of metabolite biomarkers of *S. enteritidis* in chicken meat. (A) Volcano plots of differentially abundant metabolites between the two groups. (B) OPLS-DA score plots constructed based on UHPLC-QTRAP-MS data from two groups of chicken samples. (C) Permutation test plots constructed based on UHPLC-QTRAP-MS data, (D) Column plot of OPLS-DA model permutation test results (E) Pathway analysis plots of differentially abundant metabolites from *S. enteritidis*-contaminated and control samples. (F) Coefficient distribution of LASSO analysis (G) Plot of the mean squared deviation of the tests expressed as lambda values in the LASSO analysis. (H) Biomarker score plot in LASSO analysis. (I) Hierarchical cluster heatmaps of the metabolite biomarkers.

hydroxybenzoic acid, menatetrenone, glycyl phenylalanine and 5-methyl-2′-deoxycytidine were the highest contributing factors, suggesting that they might be crucial metabolite biomarkers of *S. enteritidis* contamination in chickens.

3.7. Evaluation of metabolite biomarkers

To better evaluate the metabolic patterns of significant differences in metabolites between the *S. enteritidis* and control groups, we calculated the Euclidean distance matrix for the quantitative value of 8 metabolite biomarkers and clustered the DAMs with the complete linkage method to display the DAMs with the heatmap (Chen et al., 2022; Nie et al., 2022). As shown in Fig. 3I, the eight metabolite biomarkers showed distinct patterns between *S. enteritidis*-contaminated and control samples.

The abundance of the eight metabolite biomarkers was visualized by violin plots (Fig. 4A-F). The results indicated that anthranilic acid, l-pyroglutamic acid, 5-hydroxylysine, n,*n*-dimethylarginine, 4-hydroxybenzoic acid, and menatetrenone were significantly upregulated ($P < 0.001$) in the contamination group samples. Lan et al. identified creatinine as one of the metabolite biomarkers of *S. enteritidis*-contaminated chickens by targeted and untargeted metabolomics (Chen et al., 2023). Xu et al. found that amino acids were detected in *Salmonella* typhimurium-contaminated pork samples, and their abundance was significantly higher than that of naturally spoiled pork samples (Yun et al., 2011). Glycylphenylalanine and 5-methyl-2′-deoxycytidine were downregulated considerably in *S. enteritidis*-contaminated chickens ($P < 0.01$) (Fig. 4G-H). It is well known that changes in the contents of amino acids, nucleotides and fatty acid metabolites directly reflect fresh meat's physiological and biochemical reactions (Herranz, de la Hoz, Hierro, Fernández, & Ordóñez, 2005). It may be that bacteria preferentially utilize glycine-phenylalanine in a specific way, leading to a significant downregulation in its content (Yun et al., 2011). In the *S. enteritidis*-contaminated chicken group, glycyl phenylalanine and 5-methyl-2′-deoxycytidine were significantly lower than those in the blank control group, which may be the substrate consumed to meet the growth rate of bacteria. Compared with the control group, the contents of anthranilic acid, l-pyroglutamic acid, 5-hydroxylysine, n,*n*-dimethylarginine, 4-hydroxybenzoic acid, and menatetrenone were significantly upregulated, which could be used as new metabolite biomarkers in *S. enteritidis* contamination of chicken.

ROC curve analysis is a recognized method for evaluating marker performance (Junge & Dettori, 2018; Kamarudin et al., 2017). AUC values > 0.9 indicate excellent predictive power, and AUC < 0.5 suggests a lack of predictive power (Fu & Peng, 2017). We used ROC curve analysis to evaluate the ability of the metabolite biomarkers to predict *S. enteritidis* contamination in chicken meat. The results showed that six single metabolite biomarker ROC analysis was > 0.9(Fig. S1, Table S5), combined ROC analysis of the six metabolite biomarkers obtained an AUC value of 0.99, a sensitivity of 0.99, and a specificity of 1(Fig. 4I).

Table 1
Potential biomarkers of *S. enteritidis* contamination group.

Number	Metabolite name	Formula	VIP	P-value	Fold Change
1	Mannitol	C6H14O6	1.434758069	9.383E-05	4.62054E-07
2	Succinic acid	C4H6O4	1.433737384	4.32979E-06	648365363.6
3	Kynurenic acid	C10H7NO3	1.433298154	2.37724E-06	24245.12764
4	Maleic acid	C4H4O4	1.432905427	0.001033698	346790.0871
5	Menatetrenone	C31H40O2	1.432790535	7.64555E-06	21005.16377
6	Indole-3-butyric acid	C12H13NO2	1.432193205	2.48811E-06	2473.96526
7	Thymidine	C10H14N2O5	1.43052051	0.000372438	1.62706E-05
8	Trimethylamine *N*-oxide	C3H9NO	1.43050612	2.5934E-05	4.09718E-05
9	5-Aminoimidazole-4-carboxamide	C4H6N4O	1.429971853	0.000112447	58808.17866
10	Corticosterone	C21H30O4	1.429398434	0.0001593	4486.586987
11	D-Glucose	C6H12O6	1.425240268	2.03082E-06	0.01983839
12	Picolinic acid	C6H5NO2	1.423599374	5.91611E-06	200.6568714
13	N,*N*-Dimethylarginine	C8H18N4O2	1.422633785	1.79952E-08	14.19138523
14	Guanine	C5H5N5O	1.421966991	2.28992E-06	48.26286024
15	Uracil	C4H4N2O2	1.420487757	0.006831353	2290186.659
16	Ciliatine	C2H8NO3P	1.418718217	0.01602183	33758.75049
17	Nicotinic acid	C6H5NO2	1.418152925	0.001130555	1871.269625
18	L-Fucose-1-phosphate	C6H13O8P	1.417795006	8.66793E-05	820.7622142
19	7-Methylguanine	C6H7N5O	1.41662534	3.48466E-06	152.8167077
20	Glucaric acid	C6H10O8	1.41444064	0.00399751	8544.458288
21	L-Dopa	C9H11NO4	1.413628814	3.00973E-05	81.95100516
22	Anthranilic acid	C7H7NO2	1.411228513	1.85525E-14	3.7645379
23	L-Asparagine	C4H8N2O3	1.410276146	6.24789E-06	0.009526239
24	Pyridoxal	C8H9NO3	1.407463069	0.000545954	27.36133198
25	L-Citrulline	C6H13N3O3	1.407021099	2.82439E-05	63.26718028
26	Riboflavin	C17H20N4O6	1.406139456	2.93416E-07	13.6896795
27	N,*N*-Dimethylguanosine	C12H17N5O5	1.405163035	1.57163E-06	27.23855236
28	Glycerophosphoric acid	C3H9O6P	1.403798129	1.36605E-05	10.95715355
29	gamma-Glutamylmethionine	C10H18N2O5S	1.403459402	1.05116E-06	11.75580276
30	Pyridoxamine	C8H12N2O2	1.403412808	0.000361946	58.46075333
31	5-methyl-2′-deoxycytidine	C10H15N3O4	1.402640292	7.56459E-08	0.001366096
32	L-Aspartic acid	C4H7NO4	1.402390133	0.002091645	0.006696876
33	Adenosine-5′-diphosphate	C10H15N5O10P2	1.401339576	0.000183895	45.27943081
34	L-Ornithine	C5H12N2O2	1.396920606	6.30389E-05	32.36678766
35	Mevalonic acid	C6H12O4	1.396030878	2.47575E-05	25.0418326
36	Pyridoxine	C8H11NO3	1.395754036	0.000221665	49.83611861
37	Spaglumic acid	C11H16N2O8	1.395001021	0.00129327	34.43073183
38	Inosine diphosphate	C10H14N4O11P2	1.394520753	0.002204953	44.14924643
39	Creatinine	C4H7N3O	1.393373063	1.81653E-08	4.86851132
40	*N*-Acetylserine	C5H9NO4	1.393182868	1.95569E-06	6.966278905
41	5-Hydroxylysine	C6H14N2O3	1.392356367	1.14738E-09	3.759987963
42	*N*-Acetyl-Neuraminic Acid	C11H19NO9	1.37903078	1.98045E-08	3.994479534
43	Glycylphenylalanine	C11H14N2O3	1.375654961	5.22938E-09	0.220003373
44	*N*-Acetyl-L-alanine	C5H9NO3	1.37435207	5.66992E-08	4.026751306
45	Hypoxanthine	C5H4N4O	1.373119668	1.65315E-08	4.051638779
46	gamma-L-Glutamyl-L-valine	C10H18N2O5	1.371000259	0.010598432	260.6230856
47	Tyramine	C8H11NO	1.370563256	4.01234E-05	54069.88222
48	Chenodeoxycholic acid	C24H40O4	1.368833179	0.000112818	14.97926016
49	*N*-Acetyl-L-glutamic acid	C7H11NO5	1.368041933	0.000105327	325.0126189
50	Xanthosine	C10H12N4O6	1.36304167	0.000398997	12.09654928
51	Adenine	C5H5N5	1.362985781	0.000105068	20.46051063
52	Prostaglandin D1	C20H34O5	1.362401459	0.000661823	67.30760544
53	1-Methyladenosine	C11H15N5O4	1.362200554	0.003364024	114.6457176
54	Hydroxyisocaproic acid	C6H12O3	1.36034664	0.04932906	172.9809165
55	4-Hydroxybenzoic acid	C7H6O3	1.359998418	3.92907E-07	7.144825543
56	NAD+	C21H27N7O14P2	1.351932717	0.000510424	0.022093005
57	L-Pyroglutamic acid	C5H7NO3	1.349434881	1.2891E-10	2.69907268
58	Glycylproline	C7H12N2O3	1.34833503	1.09692E-06	3.173735866
59	D-Mannosamine	C6H13NO5	1.347892537	0.000400063	0.012350917
60	Ethanolamine	C2H7NO	1.347814745	3.3224E-05	5.354511638
61	Uridine	C9H12N2O6	1.346738358	1.00503E-06	0.045440861
62	Leucyl-Valine	C11H22N2O3	1.343813595	7.07839E-06	0.323558675
63	Cytidine	C9H13N3O5	1.343652511	9.56044E-07	0.085597858
64	Pseudouridine	C9H12N2O6	1.342818607	7.97279E-06	9.713380701
65	*N*-Acetyl-D-Glucosamine	C8H15NO6	1.339855243	2.36985E-07	0.224939005
66	*N*-Acetylcadaverine	C7H16N2O	1.339714908	0.036171832	173.1874555
67	4-Aminobutyric acid	C4H9NO2	1.337506595	0.026217497	213.3049981
68	Choline	C5H14NO+	1.337374043	7.89115E-05	5.21793706
69	2′-Deoxyuridine	C9H12N2O5	1.336473018	7.97011E-07	0.144828822
70	*N*-Acetyl-L-aspartic acid	C6H9NO5	1.33553154	0.002146278	12.71727739
71	7-Ketocholesterol	C27H44O2	1.334338097	5.22493E-06	6.140109129
72	*N*-Acetyl-S-(3-hydroxypropyl)cysteine	C8H15NO4S	1.330297992	4.55937E-07	1.828757848
73	Glycyl-L-Leucine	C8H16N2O3	1.328651144	1.57729E-05	0.179921162
74	L-2-Aminobutyric acid	C4H9NO2	1.327511216	0.005533768	18.63456763

(*continued on next page*)

Table 1 (*continued*)

Number	Metabolite name	Formula	VIP	P-value	Fold Change
75	alpha-Linolenic acid	C18H30O2	1.326139842	0.000112417	4.926472116
76	Flavin adenine dinucleotide	C27H33N9O15P2	1.323627133	0.000205276	4.896391962
77	L-Cystathionine	C7H14N2O4S	1.319942263	1.93189E-09	2.654535012
78	Cinnamoylglycine	C11H11NO3	1.315949867	2.75489E-06	2.994511028
79	O-Phospho-L-Serine	C3H8NO6P	1.313452879	3.11581E-06	2.96771749
80	3-(Methylthio)propionate	C4H8O2S	1.313208211	0.000998876	6.241782977
81	Histamine	C5H9N3	1.309563346	0.00183763	65.48478845
82	*N*-Formyl-L-methionine	C6H11NO3S	1.307848137	2.39777E-05	4.218938896
83	L-Glutamic acid	C5H9NO4	1.30301518	1.29335E-08	1.762414764
84	2-Hydroxyadipic acid	C6H10O5	1.300481551	0.000827077	5144.858879
85	Melatonin	C13H16N2O2	1.297420121	2.12188E-05	1008.863952
86	L-Leucine	C6H13NO2	1.296630553	2.77688E-09	2.261888702
87	L-Norleucine	C6H13NO2	1.296426981	6.20588E-09	1.940082859
88	UDP-D-glucose	C15H24N2O17P2	1.290602171	0.00635958	0.000328085
89	Cyclic guanosine monophosphate	C10H12N5O7P	1.290044756	0.000136796	135.1091414
90	L-Valine	C5H11NO2	1.28852505	1.85284E-07	1.889381293
91	2′-O-methylguanosine	C11H15N5O5	1.283941459	7.16523E-05	3.745936119
92	1-Aminopropan-2-ol	C3H9NO	1.282458248	0.032329825	71.56939308
93	Xylulose 5-phosphate	C5H11O8P	1.278931895	1.25124E-09	0.243036319
94	Threonylphenylalanine	C13H18N2O4	1.276975226	1.3845E-07	0.404544673
95	Nicotinamide mononucleotide	C11H15N2O8P	1.272930899	0.003418342	0.084017464
96	3-Indoleglyoxylic acid	C10H7NO3	1.268300011	0.007820213	45.71521261
97	Glutathione Disulfide	C20H32N6O12S2	1.253499529	0.000451134	3.819581596
98	Acetylcysteine	C5H9NO3S	1.248707988	4.28237E-08	2.093919506
99	S-Adenosylmethionine	C15H22N6O5S	1.247159206	0.000215715	0.21241555
100	L-Cysteine	C3H7NO2S	1.23124655	1.84451E-07	2.842135749
101	Adipic acid	C6H10O4	1.22630239	2.30237E-05	125.311738
102	5-Aminovaleric acid	C5H11NO2	1.221094373	0.024657977	81.03820863
103	Propionyl-CoA	C24H40N7O17P3S	1.214146485	7.42522E-07	1.647377151
104	Glutaric acid	C5H8O4	1.210209036	1.09544E-06	3.48239048
105	L-2-Aminoadipic Acid	C6H11NO4	1.207558998	0.000219151	4.063538278
106	D-Alanyl-D-alanine	C6H12N2O3	1.205759343	0.000173184	0.430366857
107	*N*-Acetylputrescine	C6H14N2O	1.199884851	0.048642962	27.10070181
108	2′-Deoxyguanosine-5′-diphosphate	C10H15N5O10P2	1.199674943	0.001288208	4.667291634
109	2-Methylcitric acid	C7H10O7	1.197969529	0.004120988	12.09301017
110	Gluconolactone	C6H10O6	1.196233846	0.000154923	0.393434536
111	L-Sorbose	C6H12O6	1.195844474	0.003710147	0.292961785
112	Inosinic acid	C10H13N4O8P	1.188574802	1.80515E-06	0.187904916
113	Xanthine	C5H4N4O2	1.188407068	0.001110893	5.601663038
114	gamma-Carboxyglutamic acid	C6H9NO6	1.187740368	0.000136218	2.263953602
115	Prostaglandin E2	C20H32O5	1.184632101	0.000268224	3.642569556
116	3-Methyl-2-oxovaleric acid	C6H10O3	1.182886759	0.019010194	99.23381336
117	Glutathione	C10H17N3O6S	1.182707611	0.005808601	0.183629752
118	L-alpha-Aspartyl-L-phenylalanine	C13H16N2O5	1.180942208	7.69868E-05	1.77661208
119	1,5-Anhydro-D-Glucitol	C6H12O5	1.176266411	1.06779E-05	0.445648701
120	5-Methoxytryptophan	C12H14N2O3	1.167915489	0.004907338	2215.208993
121	Thymidine-5′-phosphate	C10H15N2O8P	1.144910687	3.45438E-05	0.439154638
122	N6,N6,N6-Trimethyl-L-lysine	C9H20N2O2	1.138600632	0.002315363	3.522309034
123	L-Homoarginine	C7H16N4O2	1.137605993	0.002474977	3.62451569
124	2′-Deoxyadenosine-5′-monophosphate	C10H14N5O6P	1.137486158	0.001892718	6.557383588
125	S-Adenosyl-L-homocysteine	C14H20N6O5S	1.133398033	6.49611E-05	0.03271776
126	Thymidine-5-triphosphate	C10H17N2O14P3	1.127122701	0.000357749	0.129901022
127	L-Malic acid	C4H6O5	1.121798158	0.003454427	2.087745128
128	L-Phenylalanine	C9H11NO2	1.121361061	5.24317E-05	1.609935281
129	L-Tryptophan	C11H12N2O2	1.114002345	8.71431E-05	1.660924263
130	GDP-L-Fucose	C16H25N5O15P2	1.106374937	3.60223E-05	0.319173493
131	L-Methionine sulfone	C5H11NO4S	1.106187086	0.000942763	1.848219367
132	Acetyl coenzyme A	C23H38N7O17P3S	1.105913524	0.000544672	3.063719073
133	4-(Trimethylammonio)butanoate	C7H15NO2	1.105244256	0.000716847	1.894689877
134	Uridine diphosphate glucuronic acid	C15H22N2O18P2	1.103506325	0.001247134	0.292348798
135	Fumaric acid	C4H4O4	1.096822657	0.008593126	3.315426393
136	*N*-Acetyl-L-phenylalanine	C11H13NO3	1.095609098	1.23816E-06	8.775150616
137	Purine	C5H4N4	1.094707577	1.01475E-05	27.62362716
138	Glyceraldehyde	C3H6O3	1.087326495	1.12887E-05	0.362495542
139	alpha-Cyano-4-hydroxycinnamic acid	C10H7NO3	1.084740073	0.038191128	29.74697165
140	L-Tyrosine	C9H11NO3	1.080427694	7.42493E-06	0.361817265
141	Myristic acid	C14H28O2	1.060094679	0.004592455	2.155386068
142	2-Hydroxybutyric acid	C4H8O3	1.04696474	0.045677417	10.6794078
143	6-Hydroxyhexanoic acid	C6H12O3	1.042530969	0.000446796	2.163025171
144	L-Rhamnose	C6H12O5	1.038134132	0.000378924	2.328031551
145	Inosine	C10H12N4O5	1.031180242	0.000492776	0.275470809
146	Xylitol	C5H12O5	1.028537322	0.000285402	1.413444405
147	4-Pyridoxic acid	C8H9NO4	1.02491205	0.00372022	133.0608095
148	Fructose-6-phosphate	C6H13O9P	1.02466824	0.006414825	0.291892954
149	Imidazoleacetic acid	C5H6N2O2	1.021874572	0.0155894	3.6977364
150	Diethanolamine	C4H11NO2	1.014419281	0.000329209	0.395715998

(*continued on next page*)

Table 1 (*continued*)

Number	Metabolite name	Formula	VIP	P-value	Fold Change
151	*N*-Acetylglycine	C4H7NO3	1.012551275	0.000915519	13.9272037
152	D-Galacturonic Acid	C6H10O7	1.008584916	0.045422198	117.3735304

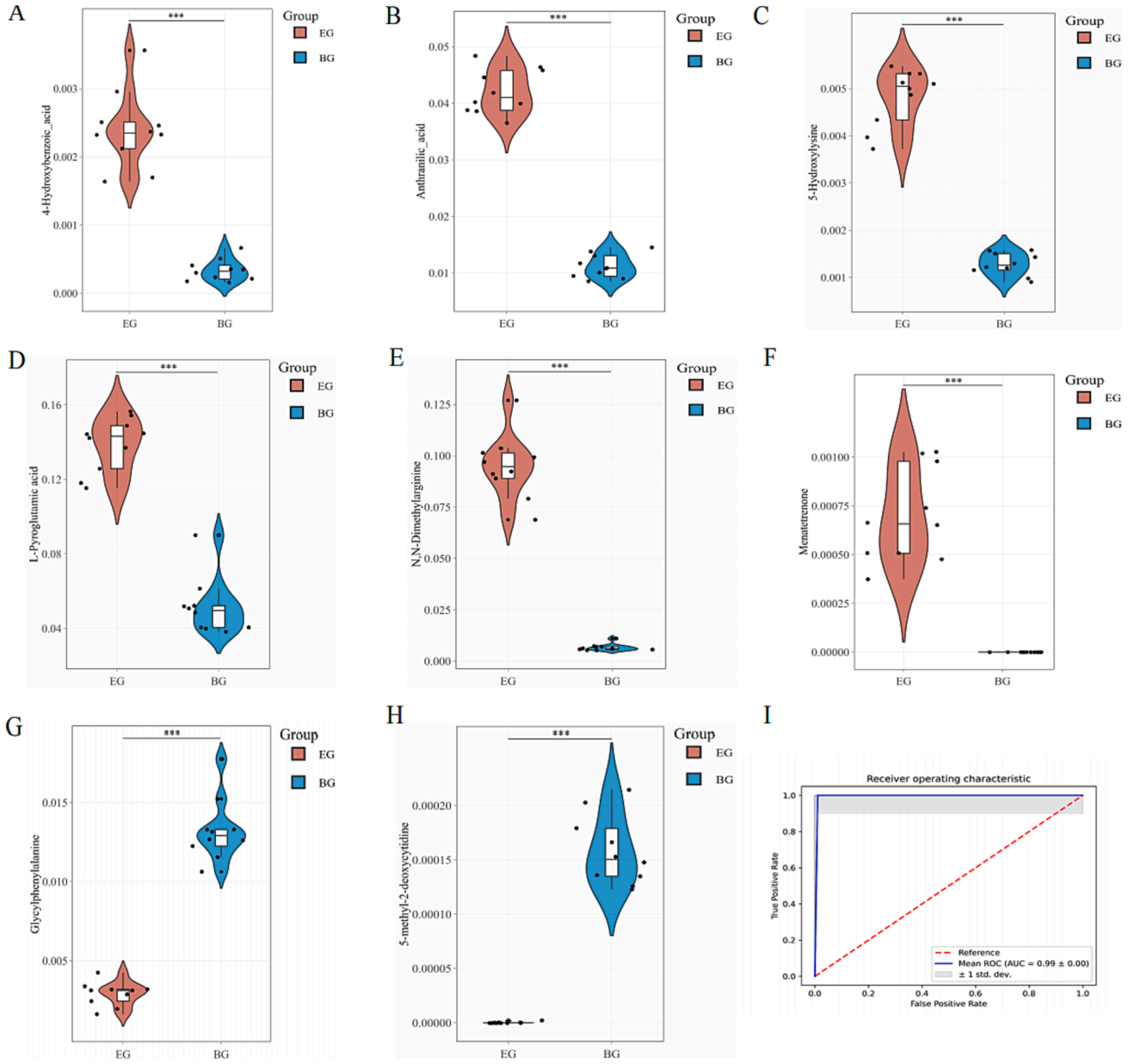

Fig. 4. Assessment of the stability of potential metabolite biomarkers of *S. enteritidis* in chicken meat (A-H) Violin plot quantitative analysis of potential metabolite biomarkers. (I) The combined ROC curve was constructed by 10-fold cross-validation of six metabolite biomarkers.

The results showed that the combination of six metabolite biomarkers had an excellent predictive ability to identify *S. enteritidis*-contaminated chicken samples.

4. Conclusion

Using UHPLC-QTRAP-MS-based targeted metabolomics, this study successfully identified 152 DAMs between chickens from *S. enteritidis*-contaminated groups and control groups. Subsequently, employing LASSO analysis, metabolite abundance change analysis and ROC curve analysis, anthranilic acid, l-pyroglutamic acid, 5-hydroxylysine, n,*n*-dimethylarginine, 4-hydroxybenzoic acid and menatetrenone were identified as metabolite biomarkers for *S. enteritidis*-contaminated chicken meat. In conclusion, the six metabolite biomarkers identified in this study provide valuable information for developing a rapid, efficient and quantitative approach to controlling *S. enteritidis* contamination of raw meat and meat products.

CRediT authorship contribution statement

Lan Chen: Conceptualization, Methodology, Software, Writing – original draft. **Tao Zhang:** Data curation, Project administration,

Validation. **Hao Ding:** Investigation, Software. **Xing Xie:** Conceptualization, Resources. **Yali Zhu:** Formal analysis. **Guojun Dai:** Resources, Project administration. **Yushi Gao:** Data curation, Resources. **Genxi Zhang:** Conceptualization, Methodology. **Kaizhou Xie:** Funding acquisition, Conceptualization, Data curation, Supervision.

Declaration of Competing Interest

The authors declare that they have no known competing financial interests or personal relationships that could have appeared to influence the work reported in this paper.

Data availability

Data will be made available on request.

Acknowledgements

This research was supported by the earmarked fund for CARS-41, the Priority Academic Programme Development of Jiangsu Higher Education Institutions (PAPD), the China Postdoctoral Science Foundation (2022M712698), the National Natural Science Foundation of China (32273011) and the Jiangsu Association for Science and Technology Youth Science and Technology Talents Support Project (TJ2023-093).

Appendix A. Supplementary data

Supplementary data to this article can be found online at https://doi.org/10.1016/j.fochx.2023.100966.

References

Algamal, Z. Y., & Lee, M. H. (2015). Penalized logistic regression with the adaptive LASSO for gene selection in high-dimensional cancer classification. *Expert Systems with Applications, 42*(23), 9326–9332. https://doi.org/10.1515/ijb-2022-0025

Antunes, P., Mourão, J., Campos, J., & Peixe, L. (2016). Salmonellosis: The role of poultry meat. *Clinical Microbiology and Infection*. https://doi.org/10.1016/j.cmi.2015.12.004

Bover-Cid, S., Izquierdo-Pulido, M., & Vidal-Carou, M. C. (2000). Influence of hygienic quality of raw materials on biogenic amine production during ripening and storage of dry fermented sausages. *Journal of Food Protection, 63*(11), 1544–1550. https://doi.org/10.4315/0362-028x-63.11.1544

Castro-Vargas, R. E., Herrera-Sánchez, M. P., Rodríguez-Hernández, R., & Rondón-Barragán, I. S. (2020). Antibiotic resistance in Salmonella spp. isolated from poultry: A global overview. *Vet. WORLD, 13*(10), 2070–2084. https://doi.org/10.14202/vetworld.2020.2070-2084

Cevallos-Cevallos, J. M., Reyes-De-Corcuera, J. I., Etxeberria, E., Danyluk, M. D., & Rodrick, G. E. (2009). Metabolomic analysis in food science: A review. *Trends in Food Science & Technology, 20*(11–12), 557–566. https://doi.org/10.1016/j.tifs.2009.07.002

Chang, C. W., Wu, H. Y., Kan, H. L., Lin, Y. C., & Liao, P. C. (2021). Discovery of spoilage markers for chicken eggs using liquid chromatography-high resolution mass spectrometry-based untargeted and targeted foodomics. *Journal of Agricultural and Food Chemistry*. https://doi.org/10.1021/acs.jafc.1c01009

Chen, C., Zheng, J., Xiong, C., Zhou, H., Wei, C., Hu, X., & Li, Z. (2022). Metabolomics characterize the differential metabolic markers between bama xiang pig and debao pig to identify pork. *Foods, 12*(1). https://doi.org/10.3390/foods12010005

Chen, Feng, Dai, Xudong, Zhou, Chang Chun, Li, Ke Xin, Zhang, Yu Juan, Lou, Xiao Ying, Cui, Wei %J Gut: Journal of the British Society of Gastroenterology. (2022). Integrated analysis of the faecal metagenome and serum metabolome reveals the role of gut microbiome-associated metabolites in the detection of colorectal cancer and adenoma. (7), 71. http://doi.org/10.1136/gutjnl-2020-323476.

Chen, L., Ding, H., Zhu, Y., Guo, Y., Tang, Y., Xie, K., & Zhang, T. (2023). Untargeted and targeted metabolomics identify metabolite biomarkers for Salmonella enteritidis in chicken meat. *Food Chemistry, 409*, Article 135294. https://doi.org/10.1016/j.foodchem.2022.135294

Dario, P., Gaston, N., & Robledo, S. (2018). Development of an electroanalytical method to control quality in fish samples based on an edge plane pyrolytic graphite electrode. Simultaneous determination of hypoxanthine, xanthine and uric acid. *Microchemical Journal: Devoted to the Application of Microtechniques in all Branches of Science, 138*, 58–64. https://doi.org/10.1021/ac900201g

Dyar, M. D., Carmosino, M. L., Breves, E. A., Ozanne, M. V., Clegg, S. M., & Wiens, R. C. (2012). Comparison of partial least squares and lasso regression techniques as applied to laser-induced breakdown spectroscopy of geological samples. *Spectrochimica Acta Part B Atomic Spectroscopy, 70*(none), 51–67. https://doi.org/10.1177/0003702820953205

Fu, L., & Peng, Q. (2017). A deep ensemble model to predict miRNA-disease association. *Scientific Reports, 7*(1), 14482. https://doi.org/10.1038/s41598-017-15235-6

He, S., Cui, Y., Dong, R., Chang, J., Cai, H., Liu, H., & Shi, X. (2022). Global transcriptomic analysis of ethanol tolerance response in Salmonella Enteritidis. *Curr Res Food Sci, 5*, 798–806. https://doi.org/10.1016/j.crfs.2022.04.011

Herranz, B., de la Hoz, L., Hierro, E., Fernández, M., & Ordóñez, J. A. (2005). Improvement of the sensory properties of dry-fermented sausages by the addition of free amino acids. *Food chemistry, 91*(4), 673–682. https://doi.org/10.1016/j.foodchem.2004.06.040

Jadhav, S. R., Shah, R. M., Karpe, A. V., Beale, D. J., Kouremenos, K. A., & Palombo, E. A. (2019). Identification of putative biomarkers specific to foodborne pathogens using metabolomics. *Methods in Molecular Biology, 1918*, 149–164. https://doi.org/10.1007/978-1-4939-9000-9_12

Jadhav, S. R., Shah, R. M., Karpe, A. V., Morrison, P. D., Kouremenos, K., Beale, D. J., & Palombo, E. A. (2018). Detection of Foodborne pathogens using proteomics and metabolomics-based approaches. *Frontiers in Microbiology, 9*, 3132. https://doi.org/10.3389/fmicb.2018.03132

Johnson, A. E., Sidwick, K. L., Pirgozliev, V. R., Edge, A., & Thompson, D. F. (2018). Metabonomic profiling of chicken eggs during storage using high-performance liquid chromatography-quadrupole time-of-flight mass spectrometry. *Analytical Chemistry, 90*(12), 7489–7494. https://doi.org/10.1021/acs.analchem.8b01031

Johnson, C. H., Ivanisevic, J., & Siuzdak, G. (2016). Metabolomics: Beyond biomarkers and towards mechanisms. *Nature Reviews. Molecular Cell Biology, 17*(7), 451–459. https://doi.org/10.1038/nrm.2016.25

Junge, M. R. J., & Dettori, J. R. (2018). ROC solid: Receiver operator characteristic (ROC) curves as a foundation for better diagnostic tests. *Global Spine Journal, 8*(4), 424–429. https://doi.org/10.1177/2192568218778294

Kamarudin, A. N., Cox, T., & Kolamunnage-Dona, R. (2017). Time-dependent ROC curve analysis in medical research: Current methods and applications. *BMC Medical Research Methodology, 17*(1), 53. https://doi.org/10.1186/s12874-017-0332-6

Lechtenfeld, O. J., Hertkorn, N., Shen, Y., Witt, M., & Benner, R. (2015). Marine sequestration of carbon in bacterial metabolites. *Nature Communications, 6*, 6711. https://doi.org/10.1038/ncomms7711

Leng, S., Zhang, X., Wang, S., Qin, J., Liu, Q., Liu, A., & Peng, J. (2022). Ion channel Piezo1 activation promotes aerobic glycolysis in macrophages. *Frontiers in Immunology, 13*, Article 976482. https://doi.org/10.3389/fimmu.2022.976482

Lindon, J. C., Holmes, E., & Nicholson, J. K. (2006). Metabonomics techniques and applications to pharmaceutical research & development. *Pharmaceutical Research, 23*(6), 1075–1088. https://doi.org/10.1007/s11095-006-0025-z

Manuel, C. J., & Danyluk, M. D. (2011). GC-MS based metabolomics for rapid simultaneous detection of Escherichia coli O157:H7, Salmonella Typhimurium, Salmonella Muenchen, and Salmonella Hartford in ground beef and chicken. *Journal of Food Science, 76*, M238–M246. https://doi.org/10.1111/j.1750-3841.2011.02132.x

Mceligot, A. J., Poynor, V., Sharma, R., & Panangadan, A. (2020). *Logistic LASSO Regression for Dietary Intakes and Breast Cancer.*. https://doi.org/10.3390/nu12092652

Nie, X., Chen, H., Xiang, L., Zhang, Y., Liu, D., & Zhao, Z. (2022). GC-TOF-MS-based non-targeted metabolomic analysis of differential metabolites in chinese ultra-long-term industrially fermented kohlrabi and their associated metabolic pathways. *Metabolites, 12*(10). https://doi.org/10.3390/metabo12100991

Parisi, A., Stanaway, J. D., Sarkar, K., & Crump, J. A. (2020). The global burden of non-typhoidal salmonella invasive disease: A systematic analysis for the Global Burden of Disease Study 2017. *International Journal of Infectious Diseases, 101*, 341. https://doi.org/10.1016/S1473-3099(19)30418-9

Pinu, F. R., Beale, D. J., Paten, A. M., Kouremenos, K., Swarup, S., Schirra, H. J., & Wishart, D. (2019). Systems biology and multi-omics integration: Viewpoints from the metabolomics research community. *Metabolites, 9*(4). https://doi.org/10.3390/metabo9040076

Regalado-Pineda, I. D., Rodarte-Medina, R., Resendiz-Nava, C. N., Saenz-Garcia, C. E., Castaeda-Serrano, P., & Nava, G. M. J. F. (2020). Three-Year Longitudinal Study: Prevalence of Salmonella Enterica in Chicken Meat is Higher in Supermarkets than Wet Markets from Mexico. 9(3). http://doi.org/10.3390/foods9030264.

Sandra, H., Brecht, D., Willy, A., Roger, C., Tim, C., Arie, H., & Robin, L. (2017). Attribution of global foodborne disease to specific foods: Findings from a World Health Organization structured expert elicitation. *PLoS One1, 12*(9), e0183641.

Sangster, T., Major, H., Plumb, R., Wilson, A. J., & Wilson, I. D. (2006). A pragmatic and readily implemented quality control strategy for HPLC-MS and GC-MS-based metabonomic analysis. *The Analyst, 131*(10), 1075–1078. https://doi.org/10.1039/b604498k

Schmidt, E. M., Escribano, D., Martinez-Subiela, S., Martinez-Miró, S., Hernández, F., Tvarijonaviciute, A., … Tecles, F. (2016). Development and validation of an assay for measurement of leptin in pig saliva. *BMC Veterinary Research, 12*(1), 242. https://doi.org/10.1186/s12917-016-0871-9

Schrimpe-Rutledge, A. C., Codreanu, S. G., Sherrod, S. D., & Mclean, J. A. (2016). Untargeted metabolomics strategies—Challenges and emerging directions. *Journal of the American Society for Mass Spectrometry, 27*(12), 1897–1905. https://doi.org/10.1007/s13361-016-1469-y

Slowinska, M., Sallem, H., Clench, M. R., & Ciereszko, A. (2018). Metabolomic analysis of white and yellow seminal plasma in turkeys (Meleagris gallopavo). *Poultry Science, 97*(3), 1059–1065. https://doi.org/10.3382/ps/pex366

Soh, C. G., & Zhu, Y. (2022). A sparse fused group lasso regression model for fourier-transform infrared spectroscopic data with application to purity prediction in olive oil blends. *Chemometrics and Intelligent Laboratory Systems, 224*, 104530-. https://doi.org/10.1016/j.chemolab.2022.104530

Song, Y., Li, W., Duan, Y., Li, Z., & Deng, L. (2014). Nicking enzyme-assisted biosensor for Salmonella enteritidis detection based on fluorescence resonance energy transfer. *Biosensors & Bioelectronics, 55*, 400–404. https://doi.org/10.1016/j.bios.2013.12.053

Trygg, J., & Wold, S. (2002). Orthogonal projections to latent structures (O-PLS). *Journal of Chemometrics, 16*(3). https://doi.org/10.1002/cem.695

Wang, K., Wang, X., Zhang, L., Chen, A., Yang, S., & Xu, Z. (2022). Identification of novel biomarkers in chilled and frozen chicken using metabolomics profiling and its application. *Food Chemistry, 393*, Article 133334. https://doi.org/10.1016/j.foodchem.2022.133334

Wen, D., Liu, Y., & Yu, Q. (2020). Metabolomic approach to measuring quality of chilled chicken meat during storage. *Poultry Science, 99*(5), 2543–2554. https://doi.org/10.1016/j.psj.2019.11.070

Wiklund, S., Johansson, E., Sjöström, L., Mellerowicz, E. J., Edlund, U., Shockcor, J. P., … Trygg, J. (2008). Visualization of GC/TOF-MS-based metabolomics data for identification of biochemically interesting compounds using OPLS class models. *Analytical Chemistry, 80*(1), 115–122. https://doi.org/10.1021/ac0713510

Wu, W., Li, J., Pan, D., Li, J., Song, S., Rong, M., … Lu, J. (2014). Gold nanoparticle-based enzyme-linked antibody-aptamer sandwich assay for detection of Salmonella Typhimurium. *ACS Applied Materials & Interfaces, 6*(19), 16974–16981. https://doi.org/10.1021/am5045828

Xia, J., & Wishart, D. S. (2016). Using Metaboanalyst 3.0 for comprehensive metabolomics data analysis. Curr Protoc Bioinformatics, 55, 14.10.11-14.10.91. http://doi.org/10.1002/cpbi.11.

Yun, X.u., Cheung, W., Winder, C. L., Dunn, W. B., & Goodacre, R. (2011). Metabolic profiling of meat: Assessment of pork hygiene and contamination with Salmonella typhimurium. *The Analyst, 136*(3), 508–514. https://doi.org/10.1039/c0an00394h

Zhang, T., Ding, H., Chen, L., Zhang, S., Wu, P., Xie, K., & Wang, J. (2021). Characterization of chilled chicken spoilage using an integrated microbiome and metabolomics analysis. *Food Research International, 144*, Article 110328. https://doi.org/10.1016/j.foodres.2021.110328

Zhang, Z., Mu, X., Shi, Y., & Zheng, H. (2022). Distinct roles of honeybee gut bacteria on host metabolism and neurological processes. *Microbiol Spectr, 10*(2), e0243821.

Zhang, Z., Yang, L., Huang, X., & Gao, Y. (2019). Metabolomics profiling of polygoni multiflori radix and polygoni multiflori radix preparata extracts using UPLC-Q/TOF-MS. *Chinese Medicine, 14*, 46. https://doi.org/10.1186/s13020-019-0268-3

Zhou, L., Cai, Y., Yang, L., Zou, Z., Zhu, J., & Zhang, Y. (2022). Comparative metabolomics analysis of stigmas and petals in chinese saffron (crocus sativus) by widely targeted metabolomics. *Plants (Basel), 11*(18). https://doi.org/10.3390/plants11182427